

## Synthesis of $\text{Cu}_x\text{O}$ ( $x = 1,2$ )/Amorphous Compounds by Dealloying and Spontaneous Oxidation Method

Zhifeng Wang, Chunling Qin, Li Liu, Lijuan Wang, Jian Ding, Weimin Zhao\*

School of Materials Science and Engineering, Hebei University of Technology, Tianjin 300130, China

Received: August 7, 2012; Revised: August 22, 2013

$\text{Cu}_x\text{O}$  ( $x = 1,2$ )/amorphous compounds have been successfully synthesized by chemical free dealloying and spontaneous oxidation method. Technological parameters, such as the acid concentration and dealloying time strongly influence the crystal type, size and morphology of copper oxide. The further study shows that with the increase of HCl concentration, the surface coverage rate of  $\text{Cu}_2\text{O}$  micro-flowers increases and the sizes of  $\text{Cu}_2\text{O}$  micro-flowers get bigger. Moreover, it is observed that cracks are formed on the etched ribbon surface and plentiful  $\text{Cu}_2\text{O}/\text{CuO}$  particles grow up from these crack walls if the dealloying time extends to long enough. Considering many fascinating properties of  $\text{Cu}_2\text{O}/\text{CuO}$  particles and the amorphous alloy carrier, potential application fields of these amazing compounds will be developed in future.

**Keywords:** dealloying, amorphous alloy,  $\text{Cu}_2\text{O}$ ,  $\text{CuO}$ , compounds

### 1. Introduction

Dealloying, which refers to the selective dissolution of one or more components out of an alloy, is superior in the fabrication of nanoporous metals with open pores owing to its high reactivity of some alloying elements and controllability of chemical reactions<sup>1</sup>. This method has been successfully adopted in the fabrication of nanoporous noble metals in different alloy systems<sup>2-4</sup>. Nowadays, some studies reveal that dealloying method can be extended to the fabrication of metal oxide nanostructures with intricate structural properties. Fascinating nanostructures, such as  $\text{Cu}_2\text{O}$  nanocubes<sup>1,5</sup>, octahedral  $\text{Fe}_3\text{O}_4$  and  $\text{Mn}_3\text{O}_4$  nanoparticles<sup>6</sup>, are successfully produced by dealloying method.

$\text{Cu}_2\text{O}$ , which is an important p-type semiconductor with a direct band gap of 2.17 eV<sup>7</sup>, has been widely studied as a promising material for applications in gas sensors<sup>8</sup>, in solar energy conversion<sup>9</sup>, as an electrode in lithium ion batteries<sup>10</sup>, as a photocatalyst for the degradation of organic pollutants<sup>11</sup> and for the decomposition of water into  $\text{H}_2$  and  $\text{O}_2$  under visible light irradiation<sup>12</sup>.  $\text{CuO}$  is a p-type semiconductor with narrow band gap of 1.2 eV<sup>13</sup>, and is known for its applications in optical switches, field emitters, gas sensors, high temperature microconductors, Li-ion battery anode materials, and chemical conversion catalysts<sup>14,15</sup>. Therefore,  $\text{Cu}_2\text{O}$  and  $\text{CuO}$  particles with different size and morphologies are highly desirable for these applications.

So far,  $\text{Cu}_2\text{O}$  and  $\text{CuO}$  have been prepared by several different methods. In our previous paper, we develop a new approach to produce  $\text{Cu}_2\text{O}$ /amorphous compounds by free dealloying Cu-based amorphous alloys and spontaneous oxidation method. In this study, we adjust the technical parameters to improve the  $\text{Cu}_2\text{O}$  surface coverage rate and produce  $\text{Cu}_x\text{O}$  ( $x = 1,2$ )/amorphous compounds by using

this method. To our knowledge, amorphous alloys are good carriers for  $\text{Cu}_x\text{O}$  ( $x = 1,2$ ) particles, because amorphous alloys exhibit high strength and high toughness. In addition, the  $\text{Cu}_x\text{O}$  ( $x = 1,2$ ) particles formed in the amorphous alloy precursor are more easier to be stored or extracted as compared to traditional chemical method. Meanwhile, the fabrication process of  $\text{Cu}_x\text{O}$  ( $x = 1,2$ ) particles are simplified in this route. The most important contribution by this work is to produce the amazing compounds with multiple properties which are hopeful to be applied in broad fields in future.

### 2. Experimental

Cu-based ingots with nominal compositions of  $\text{Cu}_{32.5}\text{Hf}_{40}\text{Al}_{7.5}$  (at%) were prepared by arc-melting Cu (99.99 mass%), Hf (99.99 mass%), and Al (99.99 mass%) metals in high-purity argon gas atmosphere and using Ti getters. Thin precursor ribbons of Cu-based alloys about 20  $\mu\text{m}$  thick and 2 mm wide were prepared by melt-spinning with a linear velocity of the copper wheel of 40 m/s. The free dealloying was performed by immersing amorphous precursor ribbons (about 20 mm long) into HCl solutions with different concentration and immersing time open to air at room temperature. The dealloyed samples were rinsed in deionized water for three times to remove the residual chemical substances and then dried in a vacuum drying oven. The microstructure and surface morphology of the dealloyed specimens were characterized by X-ray diffraction (XRD, Bruker D8, Cu-K $\alpha$  radiation) and scanning electron microscope (SEM, Hitachi S-4800), respectively.

### 3. Results and Discussion

Figure 1 shows XRD patterns of the dealloyed Cu-Hf-Al amorphous alloys in 0.5 M HCl solution for 0 h, 8 h,

\*e-mail: [wmzhao@yahoo.com](mailto:wmzhao@yahoo.com)

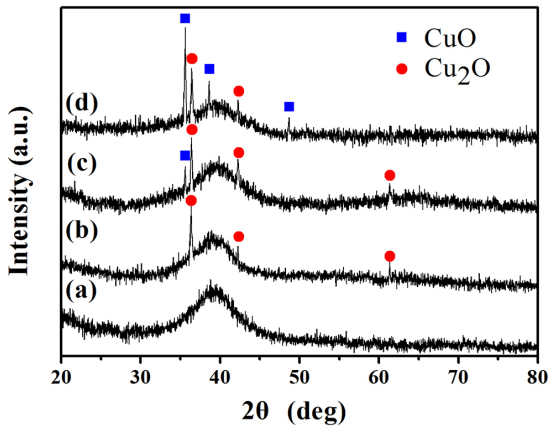


**Figure 1.** XRD patterns of dealloyed Cu-Hf-Al amorphous alloys in 0.5 M HCl solution for (a) 0 h, (b) 8 h, (c) 14 h, (d) 20 h.

14 h and 20 h, respectively. The diffraction pattern for the as-spun alloy is broad and has no Bragg peaks, indicating a single homogeneous glassy structure. The XRD patterns of the HCl treated ribbons exhibit broad halo peaks superimposed on sharp crystal peaks. These crystal peaks are match with (111), (200), (220) crystal planes of  $\text{Cu}_2\text{O}$  (JCPDS No. 05-0667) and (002), (111),  $(20\bar{2})$  crystal planes of CuO (JCPDS No.41-0254), respectively. Moreover, the existence of a broad halo peak reveals that although the surface of the sample is rich in  $\text{Cu}_2\text{O}$  and/or CuO, the inner part remains glassy structures. When the dealloying time reaches to 8 h,  $\text{Cu}_2\text{O}$  particles are synthesized on the surface of amorphous alloy. The further increasing dealloying time leads to the formation of more oxidation products of CuO instead of  $\text{Cu}_2\text{O}$ .

Figure 2 shows SEM images of the  $\text{Cu}_{52.5}\text{Hf}_{40}\text{Al}_{7.5}$  alloys immersed in HCl solution with different concentration

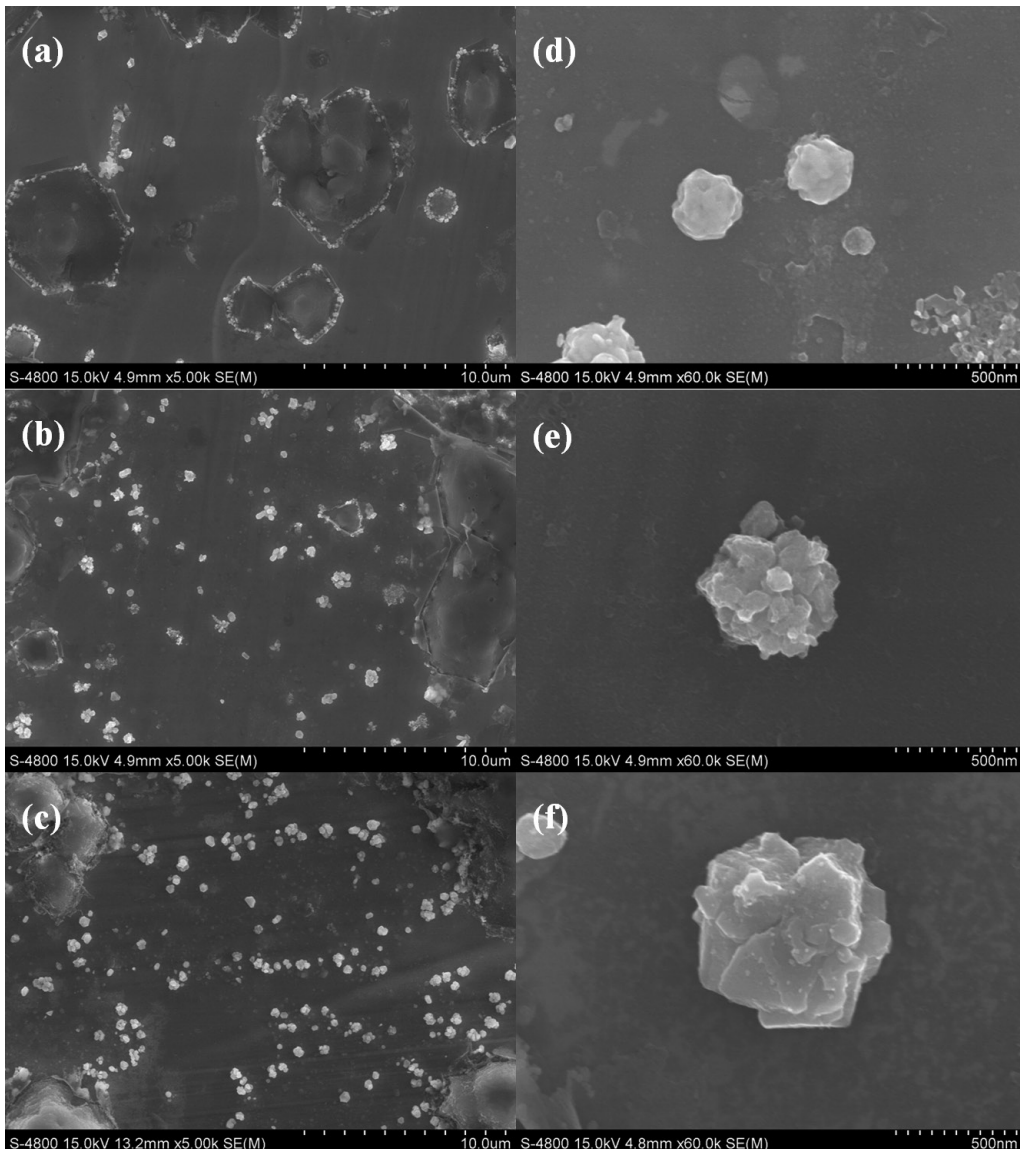


**Figure 2.** SEM micrographs of  $\text{Cu}_2\text{O}$ /amorphous compounds by etching Cu-Hf-Al amorphous alloys in different HCl solution for 8 h (a) 0.1 M, (b) 0.2 M, (c) 0.4 M. (d) ~ (f) show magnified images of (a) ~ (c), correspondingly.

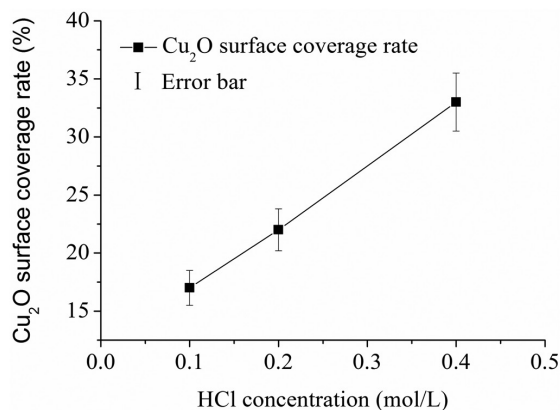


**Figure 3.**  $\text{Cu}_2\text{O}$  surface coverage rate with different HCl concentration for 8 h open to air at room temperature.

for 8 h. It is observed that  $\text{Cu}_2\text{O}$  particles formed in the amorphous alloy surface exhibit flower morphology when the dealloying time reaches to 8 h. The mean surface coverage rate of  $\text{Cu}_2\text{O}$  micro-flowers increases from 17.2% to 33.1% (as shown in Figure 3) with the increase of HCl concentration. The  $\text{Cu}_2\text{O}$  coverage rate in this paper has been improved compares with our previous study (13.9%, 0.05 M HCl for 8 h). That is because the increased HCl concentration promotes the dealloying process, including reaction speed and the reaction extent. As a result, the sizes of  $\text{Cu}_2\text{O}$  crystals gradually turn to bigger and  $\text{Cu}_2\text{O}$  crystals in regular polyhedral shapes<sup>5</sup> cannot retain but grow up to micro-flowers. On the other hand, SEM micrographs of the Cu-Hf-Al amorphous alloys dealloyed in 0.5 M HCl solution for different time are shown in Figure 4. When the dealloying time extends from 8 h to 14 h, some cracks are

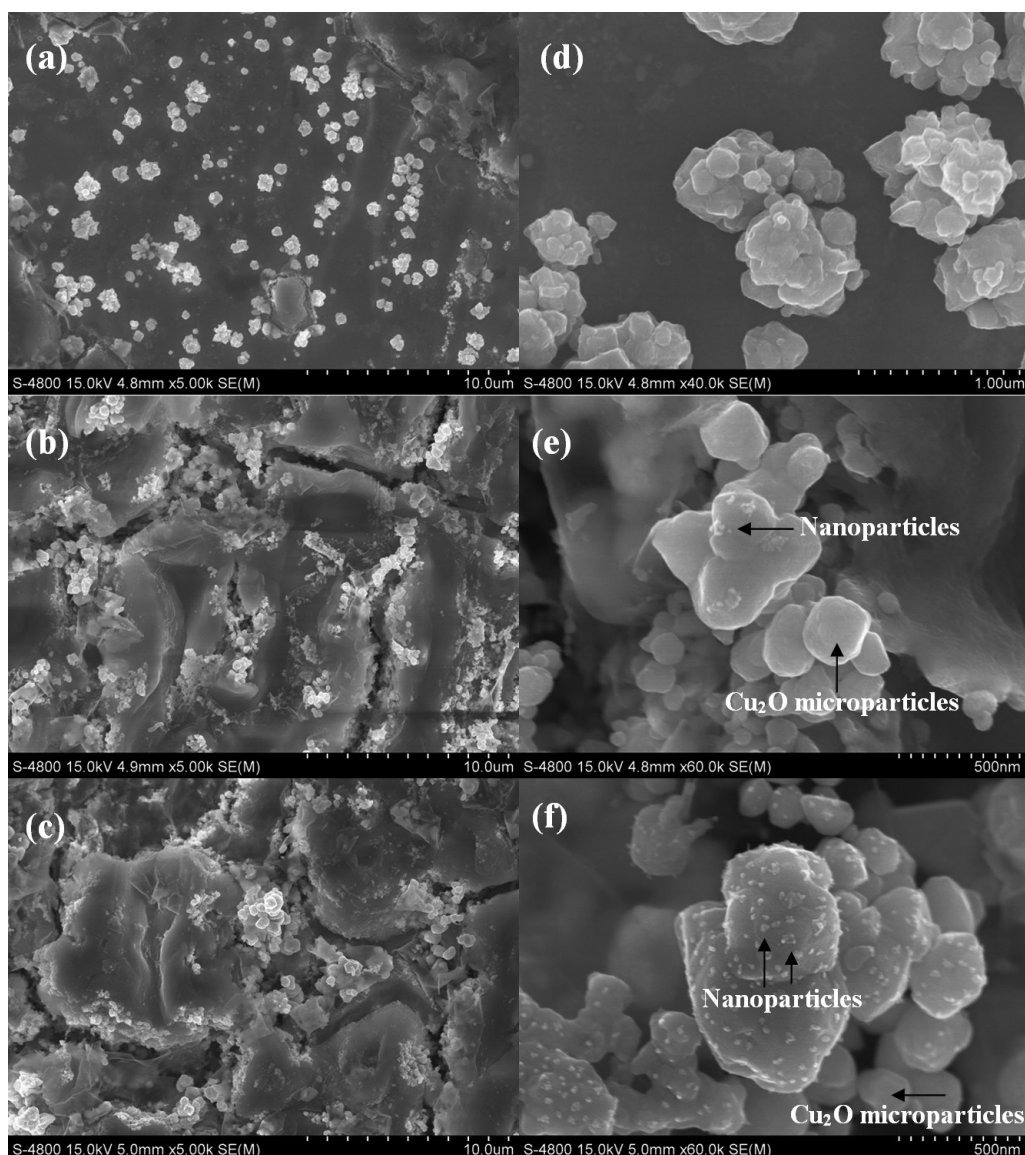


**Figure 4.** SEM micrographs of  $\text{Cu}_x\text{O}$  ( $x = 1,2$ )/amorphous compounds by etching Cu-Hf-Al amorphous alloys in 0.5 M HCl solution for (a) 8 h, (b) 14 h, (c) 20 h. (d) ~ (f) show magnified images of (a) ~ (c), correspondingly.

formed on the surface of amorphous alloys and deeper cracks are found in the ribbon dealloying for 20 h. Furthermore, it is also observed that plentiful  $\text{Cu}_2\text{O}/\text{CuO}$  particles grow up from these crack walls. The morphology of  $\text{Cu}_2\text{O}/\text{CuO}$  particles generating from crack walls is no longer flower-like, but irregular shape. The white nanoparticles denoted by black arrow in Figure 4 (e and f) grow up based on the  $\text{Cu}_2\text{O}$  micro-particles, which is a powerful evidence to represent the oxide process from  $\text{Cu}_2\text{O}$  to  $\text{CuO}$ . With the increase of the dealloying time, the mean surface coverage rate of  $\text{Cu}_x\text{O}$  ( $x = 1, 2$ ) crystals increases gradually (as shown in Figure 5). In addition, more  $\text{CuO}$  crystals can be detected from both XRD (Figure 1) and SEM (Figure 4) images.

By dealloying in HCl acidic solutions, the formation of  $\text{Cu}_2\text{O}$  and  $\text{CuO}$  on the ribbon surface is probably through the following process: First, the thin oxidized surface layer of the Cu-Hf-Al alloy is removed in the acidic electrolyte and fresh alloy layer forms on the alloy surface. Subsequent, the constituent element of the alloy are selectively dissolved into

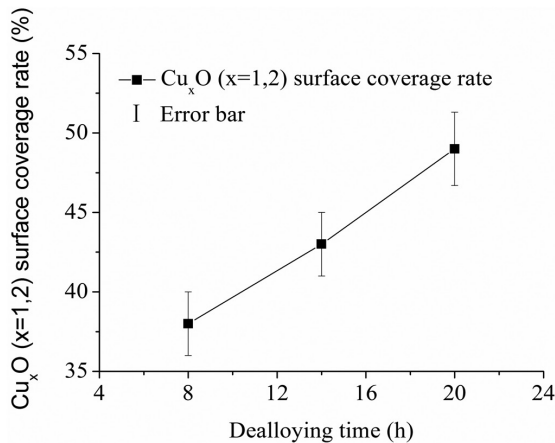


**Figure 5.**  $\text{Cu}_x\text{O}$  ( $x = 1, 2$ ) surface coverage rate with different dealloying time in 0.5 M HCl solution open to air at room temperature.

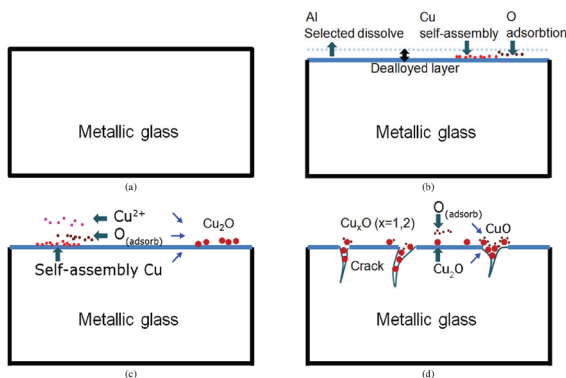


**Figure 6.** Formation schematic for  $\text{Cu}_x\text{O}$  ( $x = 1, 2$ )/amorphous compounds.

the solutions to form  $\text{Cu}^{2+}$  cations along with the other alloy elements cations<sup>1</sup>. Meanwhile the oxygen dissolved in the electrolyte also adsorbs on the fresh alloy surfaces. During the dissolution and adsorption process,  $\text{Cu}^{2+}$  cations react with metallic Cu to form  $\text{Cu}^+$  through a disproportionation reaction, these  $\text{Cu}^+$  cations are unstable and will rapidly react with the  $\text{O}-\text{O}_{(\text{adsorb})}$  to form  $\text{Cu}_2\text{O}$ . As a result, the  $\text{Cu}_2\text{O}$  particles are formed through the disproportionation reduction of metallic Cu and  $\text{Cu}^{2+}$  accompanied by surface adsorbed oxygen. If the dealloying time is long enough,  $\text{Cu}_2\text{O}$  will further react with adsorbed oxygen in acidic conditions to form the final oxidation product  $\text{CuO}$ .

A formation schematic for  $\text{Cu}_x\text{O}$  ( $x = 1, 2$ )/amorphous compounds is illustrated in Figure 6. Once the amorphous ribbon (Figure 6a) is immersed in HCl solution, the dealloying process begins. Because of the metal reactivity  $\text{Al} > \text{Cu} > \text{Hf}$  in dilute HCl solution, in principle Al and Cu elements will be selectively dissolved during dealloying process. However, the dissolution rate of Al element is much higher than that of Cu element. As a result, the ribbon retains its main part in dilute HCl solution and parts of Al elements on ribbon surface are selectively dissolved in the solution (Figure 6b). On the other hand, Cu atoms in dealloyed layer undergo self-assembly process on sample surface. It is, therefore, concluded that  $\text{Cu}_2\text{O}$  particles in the etched alloy surface are formed as a result of the disproportionation reduction of metallic Cu and  $\text{Cu}^{2+}$  accompanied by surface adsorbed oxygen (Figure 6c). If the dealloying time is extended to long enough, etching in local area speeds up. Then cracks are formed on the etched ribbon surface and plentiful  $\text{Cu}_2\text{O}/\text{CuO}$  particles grow up from these crack walls (Figure 6d).

## 4. Conclusions

$\text{Cu}_x\text{O}$  ( $x = 1, 2$ )/amorphous compounds were successfully synthesized by chemical dealloying and spontaneous oxidation method in HCl solutions. With the increase of HCl concentration, the volume fraction of  $\text{Cu}_2\text{O}$  micro-flowers improves and the size of  $\text{Cu}_2\text{O}$  micro-flowers gets bigger. The increasing dealloying time leads to the formation of more oxidation products of  $\text{CuO}$  instead of  $\text{Cu}_2\text{O}$ . In addition, it is noticed that cracks are formed on the etched ribbon surface and plentiful  $\text{Cu}_2\text{O}/\text{CuO}$  particles grow up from these crack walls when the dealloying time extends to long enough.  $\text{Cu}_2\text{O}/\text{CuO}$  particles possess many useful properties, while amorphous alloys have high strength, high toughness, and are good carriers for these oxide particles. These amazing compounds with multiple properties are hopeful to be applied in broad fields in future.

## Acknowledgments

This work is financially supported by the “100 Talents Project” of Hebei Province, China (E2012100009) and Natural Science Foundation of Hebei Province, China (E2012202017, E2010000057).

## References

1. Chen LY, Yu JS, Fujita T and Chen MW. Nanoporous copper with tunable nanoporosity for SERS applications. *Advanced Functional Materials*. 2009; 19:1221-1226. <http://dx.doi.org/10.1002/adfm.200801239>
2. Scaglione F, Gebert A and Battezzati L. Dealloying of an Au-based amorphous alloy. *Intermetallics*. 2010; 18:2338-2342. <http://dx.doi.org/10.1016/j.intermet.2010.08.005>
3. Su LS and Gan YX. Nanoporous Ag and Ag-Sn anodes for energy conversion in photochemical fuel cells. *Nano Energy*. 2012; 1:159-163. <http://dx.doi.org/10.1016/j.nanoen.2011.08.002>
4. Luo XK, Li R, Liu ZQ, Huang L, Shi MJ, Xu T et al. Three-dimensional nanoporous copper with high surface area by dealloying Mg-Cu-Y metallic glasses. *Materials Letters*. 2012; 76:96-99. <http://dx.doi.org/10.1016/j.matlet.2012.02.028>
5. Wang ZF, Qin CL, Zhao WM and Jia JQ. Tunable Cu<sub>2</sub>O nanocrystals fabricated by free dealloying of amorphous ribbons. *Journal of Nanomaterials*. 2012; Article ID 126715. <http://dx.doi.org/10.1155/2012/126715>
6. Xu CX, Wang RY, Zhang Y and Ding Y. A general corrosion route to nanostructured metal oxides. *Nanoscale*. 2010; 2:906-909. PMID:20648285. <http://dx.doi.org/10.1039/b9nr00351g>
7. Kuo CH and Huang MH. Fabrication of truncated rhombic dodecahedral Cu<sub>2</sub>O nanocages and nanoframes by particle aggregation and acidic etching. *Journal of American Chemical Society*. 2008; 130:12815-12820. PMID:18761449. <http://dx.doi.org/10.1021/ja804625s>
8. Zhang JT, Liu JF, Peng Q, Wang X and Li YD. Nearly monodisperse Cu<sub>2</sub>O and CuO nanospheres: preparation and applications for sensitive gas sensors. *Chemistry of Materials*. 2006; 18:867-871. <http://dx.doi.org/10.1021/cm052256f>
9. Mahalingam T, Chitra J, Ravi G, Chu J and Sebastian P. Characterization of pulse plated Cu<sub>2</sub>O thin films. *Surface & Coatings Technology*. 2003; 168:111-114. [http://dx.doi.org/10.1016/S0257-8972\(03\)00211-1](http://dx.doi.org/10.1016/S0257-8972(03)00211-1)
10. Poizoy P, Laruelle S, Grugeon S, Dupont L and Trascon J. Nano-sized transition-metal oxides as negative-electrode materials for lithium-ion batteries. *Nature*. 2000; 407:496-499. PMID:11028997. <http://dx.doi.org/10.1038/35035045>
11. Kumar R, Mastai Y, Diamant Y and Gedanken A. Sonochemical synthesis of amorphous Cu and nanocrystalline Cu<sub>2</sub>O embedded in a polyaniline matrix. *Journal of Materials Chemistry*. 2001; 11:1209-1213. <http://dx.doi.org/10.1039/b005769j>
12. Hara M, Kondo T, Komoda M, Ikeda S, Kondoa JN, Domen K et al. Cu<sub>2</sub>O as a photocatalyst for overall water splitting under visible light irradiation. *Chemical Communications*. 1998; (3):357-358. <http://dx.doi.org/10.1039/a707440i>
13. Liu YL, Liao L, Li JC and Pan CX. From copper nanocrystalline to CuO nanoneedle array: synthesis, growth mechanism, and properties. *Journal of Physical Chemistry C*. 2007; 111:5050-5056. <http://dx.doi.org/10.1021/jp069043d>
14. Jiang XC, Herricks T and Xia YN. CuO nanowires can be synthesized by heating copper substrates in air. *Nano Letters*. 2002; 2:1333-1338. <http://dx.doi.org/10.1021/nl0257519>
15. Grugeon S, Laruelle S, Herrera-Urbina R, Dupont L, Poizot P and Tarascon J. Particle size effects on the electrochemical performance of copper oxides toward lithium. *Journal of The Electrochemical Society*. 2001; 148:A285-A292. <http://dx.doi.org/10.1149/1.1353566>